Proceedings of the 2016 IEEE/SICE International Symposium on System Integration, Sapporo Convention Center, Sapporo, Japan, December 13-15, 2016

Effects of the Slope on the Motion of Spherical RollRoller Robot

Seyed Amir Tafrishi[1], Mikhail Svinin [2], Esmaeil Esmaeilzadeh [3]

Abstract— **In this paper, the effect of the slope on the locomotion of a spherical mobile robot named RollRoller is investigated under simulation. We analyze the robot motion up to 30 degrees of the slope inclination. The analysis is conducted for different conditions depending on the torque input and algorithmic motion planning. Oak fiber is chosen as the material of the inclined surface material, and the spherical shell of the robot is made of plastic. It is shown that RollRoller can move in different physical manners. As the velocity of the driving mass (the core) increases, certain series of jumping impulses take place because of predominant angular momentum. This pattern can support the motion of the sphere with accelerating climb in vertical axis. However, algorithmic-base position control of the RollRoller can prevent certain circular jumping impulses.**

NOMENCLATURE

γ, θ	Angular motion of the core and sphere.
m_c	Core mass (driving mass).
M_s	Robot's total mass except m_c.
ϕ	Angle of the slope.
$D1$	Piston diameter of cylinder.
$D2$	Rod diameter of cylinder.
r_c, r_d	Radius of the core and distance from center of sphere to center of core.
F_{LA}	Input force of linear actuator.
F_{c_T}	Produced force to the core
$F_{c_{Max}}$	Maximum required force to move the core in top-most gravitational point.
F_p	Force from sphere's center to massless pusher.
A_c	Projection of core area.
$\triangle P$	Pressure difference of bottom and top of core inside the pipe.
η_θ	Angular constraint of the sphere in GB activation location.
η_γ	Angular constraint of the core in GB activation location.
L_t, L_s	Traveled distance of robot respect to slope and slope total length.
R_s	Ratio of distance traveled respect to slope to the total slope distance.

I. INTRODUCTION

Spherical mobile robots represent a promising type of unconventional, single-wheel vehicles. The symmetrical shape and internal actuation of these robots let them to be a superior choice for future terrain exploration, particularly for hazardous or aggressive environments [2], [3]. Their outstanding characteristics made them the subject of many case studies in recent decades. The basic inspiration to research these models began with the nature investigation [1]. The analysis of spherical robot began with Halme et al [4] who used torque-reaction driving principle. Similar actuation methods were also proposed to drive the spherical shell [5], [6]. Other driving principles include the use of gravity and mass-imbalance [7] and angular momentum [8], [9]. It should be noted that rolling robots based on combined driving principles were also developed [10]–[12].

In spherical mobile robots, traveling on inclined plane or on uneven terrains is a big challenge, especially when there is a slippage on the plane. Yu et. al. designed and verified under simulation a controller for a pendulum-driven spherical robot to climb 10^o inclininationn without slippage [13]. The performance of two orthogonal motors by using torque-reaction actuation scheme was investigated in [14]. It was concluded that robot was able to overcome very small inclination angles. [15] had a look at a spherical robot falling from incline. In these studies, robots were only able to challenge slopes around 10^o without slippage.

In this paper, we deal with a robot named RollRoller. Its functional capabilities in propulsion on a horizontal plane were studied in [16], [17]. This spherical robot combines three three driving principles (gravitational, angular momentum, and torque-reaction) via hydraulic base fluid circulation. The fluid circulation produces required force to move a spherical movable mass, named core, inside pipes in order to create total sphere displacement.

In this work, the climb of RollRoller on the inclined plain is studied with 0^o to 30^o slope angles. The RollRoller model is studied in Adams/View simulation software. We include certain level of slippage due to oak surface material on the plain. The robot performance is evaluated in two steps. In the first one, it is done by using basic actuation with three different torque inputs (low, intermediate and high). In the second one, a position control algorithm is designed to ameliorate the performance of RollRoller motion.

This paper is organized as follows. A general overview of RollRoller is placed in Section II. In Section III, methods to move the robot on the low friction inclined plain are described. Simulation results and the evaluation of the robot performance are analyzed in Section IV. Section V concludes our work.

II. ROLLROLLER ROBOT OVERVIEW

RollRoller robot [16], [17] creates its movement by combining three driving principles, the gravitational imbalance, the change of the angular momentum, and the production of

[1]Seyed Amir Tafrishi was with Department of Automation and Control Systems, University of Sheffield, Sheffield , UK amirtafrishi@yahoo.com

[2]Mikhail Svinin is with Mechanical Engineering Department, Faculty of Engineering, Kyushu University, Fukuoka, Japan svinin@mech.kyushu-u.ac.jp

[3]Esmaeil Esmaeilzadeh is with the faculty of Mechanical Engineering, University of Tabriz as Emeritus Professor and the Mechanical Engineering, Islamic Azad University of Tabriz, Tabriz , Iran as full-time Professor esmzadeh@tabrizu.ac.ir

978-1-5090-3329-4/16/$31.00 ©2016 IEEE

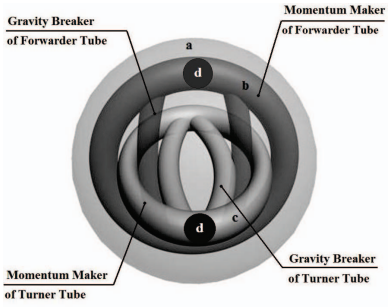

Fig. 1. a. Spherical shell, b. forwarder tube, c. turner tube. d. copper core.

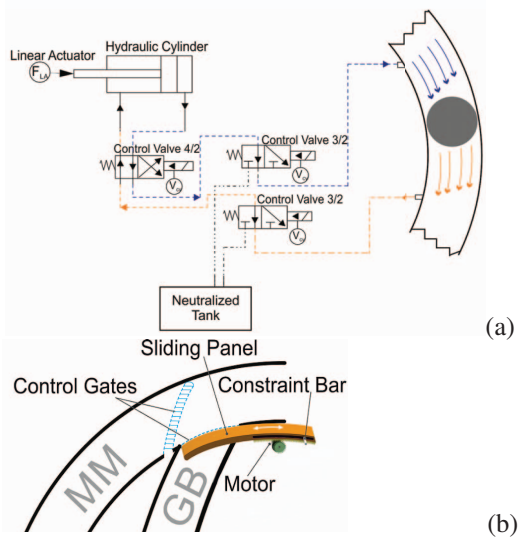

Fig. 2. (a) Schematic of internal driving unit (b) Sliding control gates.

reaction torques. The necessary driving forces are produced by displacing the cores inside the sphere via pipes as Fig. 1. The cores are movable spherical masses composed of high density metallic materials located in two tube passages. The robots leading tubes for carrying the core are named in accordance with their roles. The forwarder tube is a vertical structure that consists of circular and elliptic pipes. The horizontal compact structure, perpendicular to the forward tube, is called turner tube. Instead of circular ring in forwarder tube, the turner tube contains elliptic rings. Fundamentally, the forward/backward motion is realized via the forwarder tube. The turner tube also supports the motion by carrying its core to the corner locations. This tilts the sphere to create angular turning. The gravitational effect and the change of the angular momentum are realized by passing the core through momentum maker (MM) pipes. Also, gravity breaker (GB) pipes can cancel certain forces, such as jumping action due to angular momentum, or act as a factor to produce torque-reaction force.

In this study, the turner tube is deactivated since the climb action of the robot takes place in 2D. The internal driving unit in Fig. 2(a) produces fluid circulation from hydraulic cylinders integrated with control valves and linear actuator to push the core. Control gates are placed between intersection of GB and MM pipes and their tasks are fluid flow and core location control [see Fig. 2(b)].

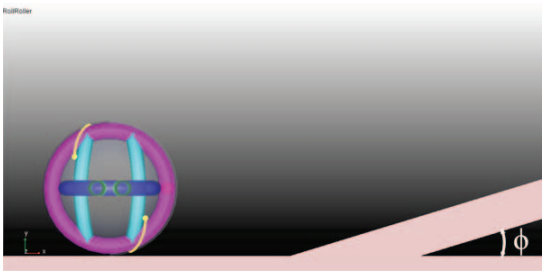

Fig. 3. Schematic space of RollRoller's locomotion simulation.

As shown in [16], [17], to overcome the instability and create a motion of high efficiency, the ration of the mass of the core, m_c, to the total mass of the sphere, M_s, should be limited as

$$\frac{1}{10} \leq \frac{m_c}{M_s} < \frac{1}{3}. \tag{1}$$

III. Locomotion on Slope

RollRoller locomotion's characteristics in slope are evaluated in the range of $0^o \leq \phi \leq 30^o$ (see Fig. 3). In our analysis, two methods of actuation, basic and hybrid, are considered. In the basic actuation, we consider the robot to move by three torque inputs (low, intermediate and high) toward the core. The driving force corresponding to the low torque input is extracted from F_{c_T}, which help us to approximately satisfy minimum requirement to move the core inside the pipe. It is established as follows,

$$F_{c_T} = F_{c_{Max}} - \delta F, \tag{2}$$

where

$$F_{c_T} = 8 r_c^2 F_{LA} [\frac{2D_1^2 - D_2^2}{D_1^2 (D_1^2 - D_2^2)}] \tag{3}$$

is the produced active force to the core from the pressure differences with linear actuator integration inside the internal driving unit, and

$$F_{c_{Max}} = m_c g + \triangle P A_c \tag{4}$$

is the maximum required force to carry the core in the topmost gravity effect. Equation (2) is derived in [16], [17]. As the linear actuator connecting rode moves to create fluid pressure circulation inside cylindrical tank of hydraulic, the created active pressure on the core tries to overcome the maximum gravity and minimum pressure difference requirement. There is no surface friction between the core and pipe surfaces due to superfluid flow.

From the equation (2), it is expected that the core is climbing up to upper half of the sphere in which δF is the small-scale value to keep the low torque input category applicable. δF is zero (for low input) when there is a solo cylinder with a constant linear actuator velocity. This value increases as the number of involved cylinders and the actuation characteristics are varied.

$$F_{c_T} \geq F_{c_{Max}}. \tag{5}$$

In simulations, the intermediate and high input torques ($\delta F > 0$) are the values that move the core with capability of

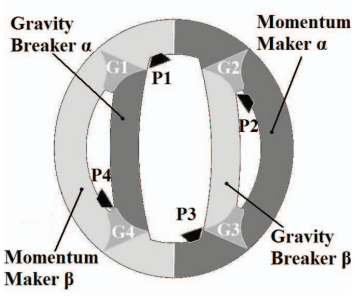

Fig. 4. Forwarder tube's partition definition for hybrid algorithm. Note: G_N and P_N are the location of standard gates and inflow ports.

satisfying complete circulation by equation (5). These forces are assumed to have value that prevent the RollRoller model to exceed reality of simulation in high velocities. In the basic actuation, we study RollRoller in both three input forms with circulating the core inside only MM. Furthermore, the hybrid actuation method is evaluated by using the intermediate stage of input.

The Adams/View simulator is used to evaluate the RollRoller performance on the slope. The Adams/View simulator can conveniently parametrize the model of RollRoller. This software uses a model of the robot imported from Solidworks software. The kinematics and nonlinear dynamics equations of RollRoller are then solved by Adams/Solver. In order to create an input torque to the core, hydraulic-base actuation is replaced with elliptic massless-pendulum pusher. Due to the fact that we consider our locomotion surface on the oak material on slope to the sphere's plastic frame, the static and dynamic friction factors are estimated as 0.6 and 0.3, respectively. In equation (1), M_s is 1 kg and m_c is 0.25 kg. The geometric size ratio of the core to the sphere is 0.096. The friction between core and pipe surfaces is ignored. The length of slope is considered to be 5 m.

In the basic actuation, the input torques are estimated by using equations (2) and (5) by using torque-force relationship $F\,r$. They are set as follows: low $\tau = 0.031$ N·m , intermediate $\tau = 0.046$ N·m and high $\tau = 0.051$ N·m.

To decrease jumping impulses observed in the basic actuation method, we introduce hybrid actuation. The main function of this control is to bring in the GB pipes in locomotion. To establish the hybrid actuation, first the Adams/View simulator's nonlinear model is exported to the Matlab Simulink space. The Adams/View block has three inputs from two gates (G1 and G2) and input force to the pendulum pusher. Also, five main outputs are related to X, Y, Z displacement, core angular locomotion (γ) and sphere angular locomotion (θ). The designed algorithm takes θ and γ locations and creates relative gate controls for G1 and G2.

The hybrid model for climbing the slope is demonstrated in Fig. 4. By using the gates G1 and G3 the control system lead the core to the GB in each region (i.e. α and β). Each of α and β regions are consist of one momentum maker and one GB pipe to lead the core during forward locomotion [17]. Note that due to the use of forward locomotion, the G2 and G4 related to the backward motion are ignored in our simulations. The algorithm functions for hybrid simulation are re-designed in [17]. The general forward locomotion is illustrated in Algorithm 1. The domain of feasible angles is

Algorithm 1 Hybrid Locomotion

procedure RIGHT DIRECTION MOTION($\theta, \dot{\theta}, \gamma, \dot{\gamma}$)
  Let γ's location determine the region S ▷ S is α/β
  while $0 < \dot{\gamma} \leq \dot{\theta}$ **do**
    Keep the core moving in MM of region S
  end while
  while $\dot{\theta} < \dot{\gamma}$ **do**
    if $-k\pi - \frac{\pi}{\eta_\gamma} < \gamma \leq -k\pi + \frac{\pi}{\eta_\gamma}$ and $k\pi + \frac{\eta_\theta \pi - \pi}{\eta_\theta} \leq \theta \leq k\pi + \frac{\eta_\theta \pi + \pi}{\eta_\theta}$ **then**
      Pass the core from GB of region S
    else
      Keep core moving in MM of region S
      if $(2k+1)\pi\theta \approx \gamma$ **then**
        Pass the core through the GB of region S
        Switch the region S
        return 3
      end if
    end if
  end while
end procedure

constrained as follows.

$$\begin{aligned}\{\cos(\theta) \leq -0.7 \ \wedge \ \sin(\theta) \geq -0.3 \ \wedge \ \dot{\theta} \geq 0 \ \wedge \\ \dot{\gamma} \leq 0 \ \wedge \ \cos(\gamma) \geq 0.6 \ \sin(\gamma) \leq 0.4 \ \} \ \vee \\ \{\cos(\theta) \geq 0.7 \ \wedge \ \sin(\theta) \leq 0.3 \ \wedge \ \dot{\theta} \geq 0 \ \wedge \\ \dot{\gamma} \leq 0 \ \wedge \ \cos(\gamma) \leq -0.6 \ \wedge \ \cos(\gamma) \geq -0.4\} \quad (6)\end{aligned}$$

$$\begin{aligned}\{|\cos(|\gamma|)| \leq 0.98 \ \wedge \ \sin(|\gamma|) \leq 0\} \vee \\ \{|\cos(|\gamma|)| \leq 0.98 \ \wedge \ \sin(|\gamma|) \geq 0\} \quad (7)\end{aligned}$$

In (6), the constraint section for sphere and core angles is expanded in order to activate the gates earlier than the core arrival to MM and GB intersections. The values of η_θ and η_γ are 4 and 1.125, respectively. By using equation (7), the algorithm keeps the control gates in their current form which is taken place in equation (6) until the next step loop.

IV. Results and Discussion

A. Basic Actuation

The displacement of the robot along Y and X axis are plotted in Fig. 5 low input torque ($\tau = 0.031$ N·m) for different slope angles. As can be seen, the inclination angles up to $\phi = 12^o$ are convenient to travel the whole slope. Interestingly, after 12^o slope the robot can not maintain its current location for highest pick that can be achieved. Also, as the degree increases from 0^o, the travel time increases proportionally. This form of torque input basically depends on the gravitational imbalance. Therefore, it can be comparable to the fundamental behavior of the pendulum driven models [4], [5], [7], [10]–[12], [18].

Next, we the simulation results for intermediate torque input ($\tau = 0.046$ N·m), are presented in the Fig. 6. A wavy

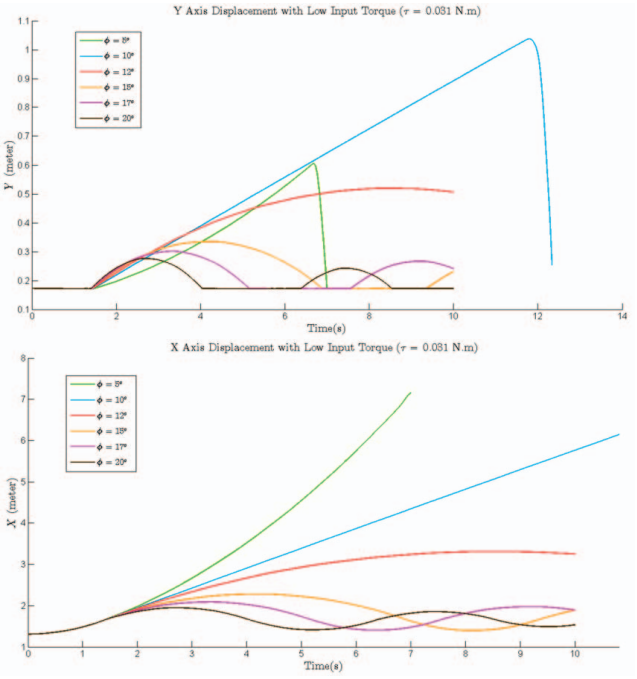

Fig. 5. Y and X axis locomotion when input torque is low.

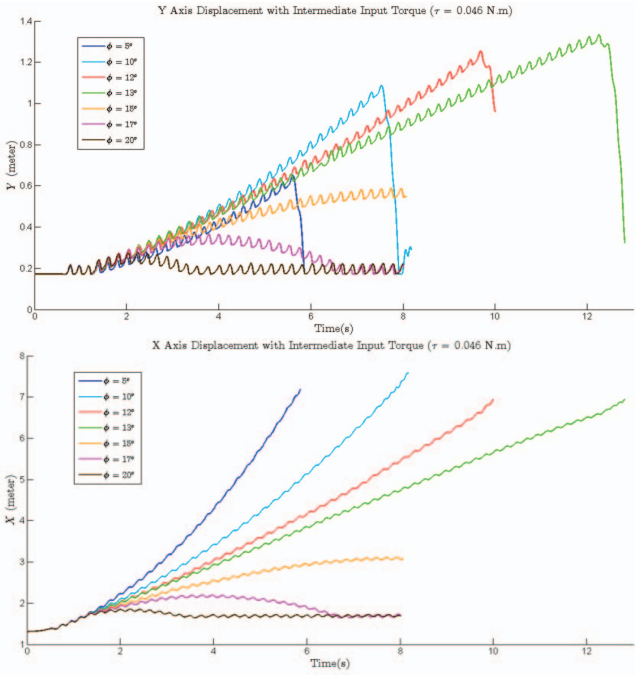

Fig. 6. Y and X axes locomotion when input torque is intermediate.

form the robot motion is appeared on along the Y axis. Behind these swings, the essential role of angular momentum is lying. While the core passes the upper half of the sphere (instability region for other previous models [4], [18]), it creates jumping impulses. This effect is proportional to the core input force. As it is obvious from Fig. 6, RollRoller follows stable locomotion along the slope. Also, this motion pattern acts as a booster to achieve a great deal of the slope climbing till 15^o. The RollRoller begins to maintain, via integrating the

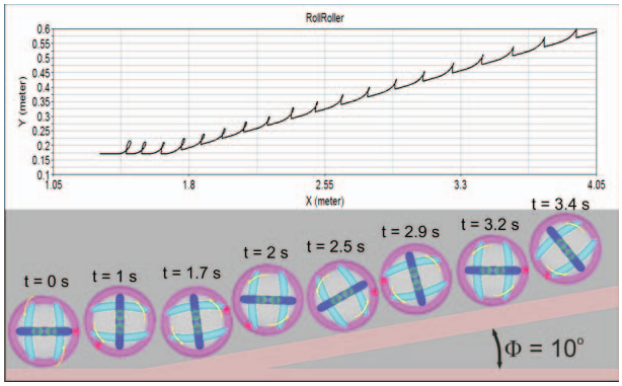

Fig. 7. The RollRoller jumping impulses effect in simulation.

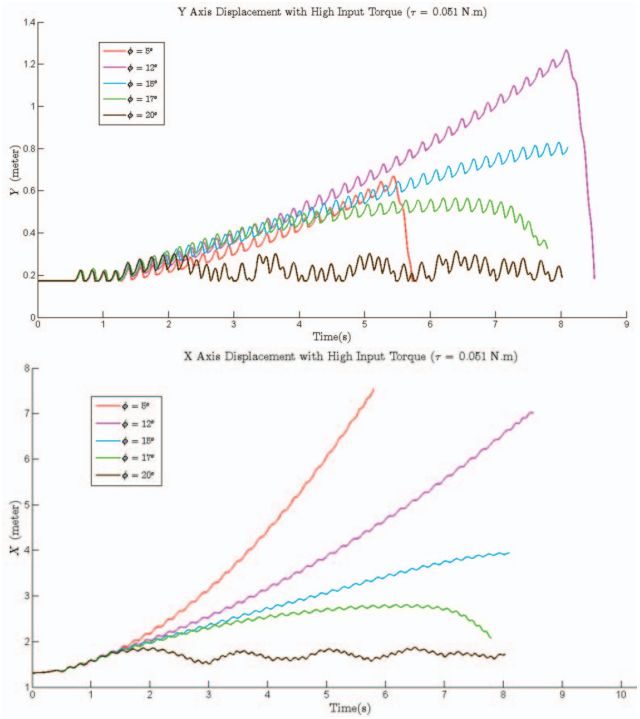

Fig. 8. Y and X axes locomotion when input torque is high.

angular momentum and gravitational imbalance, its highest location more often. As the slope angle increases to 20^o, the robot can only carry itself to the maximum distance of Y = 0.21 m and X = 1.8 m. To illustrate the jumping impulses, we plot the RollRoller in X-Y axes in Adams environment for $\phi = 10^o$ slope angle (see Fig. 7).

Next, we examine the robot behavior for the high torque input $\tau = 0.051$ N·m (high case). The simulation results are presented in Fig. 8. It can be observed that the amplitudes and the repetition frequency of all the waves are increased. As a result, the increased energy cause to rise in Y and X travel distances. In addition, as can be seen from the results, the critical slope angle for keeping the sphere in the highest travel distance is changed from 15^o to 17^o. Nevertheless, the fluctuation becomes stronger in higher than 17^o degrees.

In the Fig. 9, we summarize the locomotion performance of RollRoller in traveling a length ratio on the plain slope in

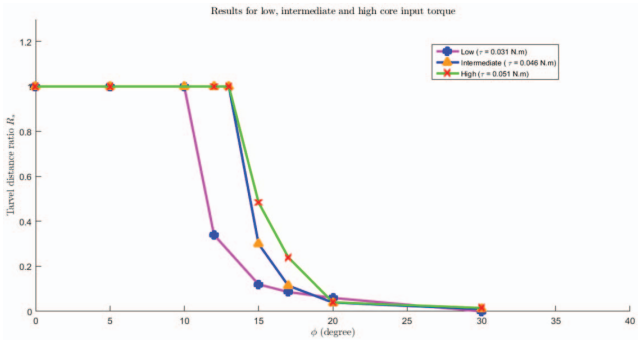

Fig. 9. Travel ratio versus the slope angles.

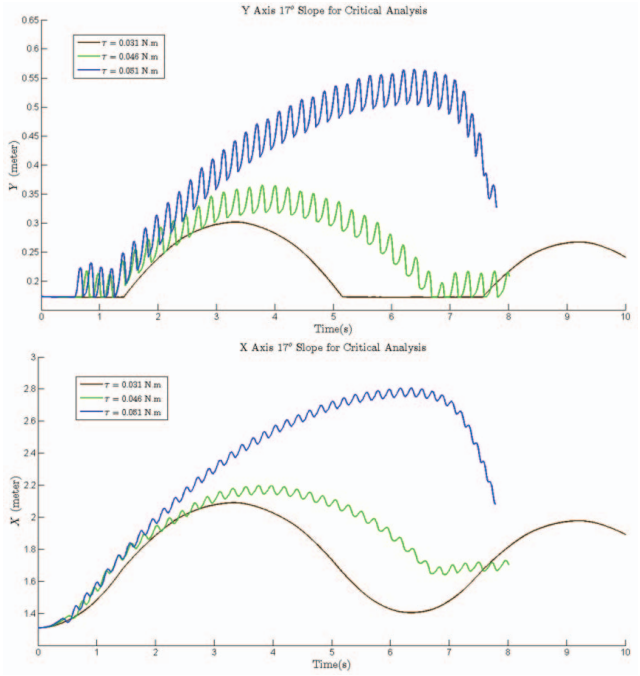

Fig. 10. Critical Analysis of 17^o slope.

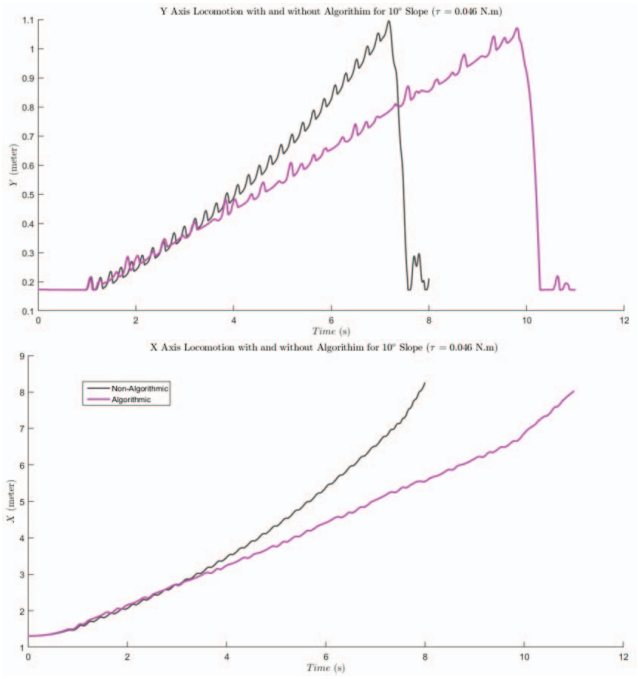

Fig. 11. Y and X axes locomotion when input torque is intermediate.

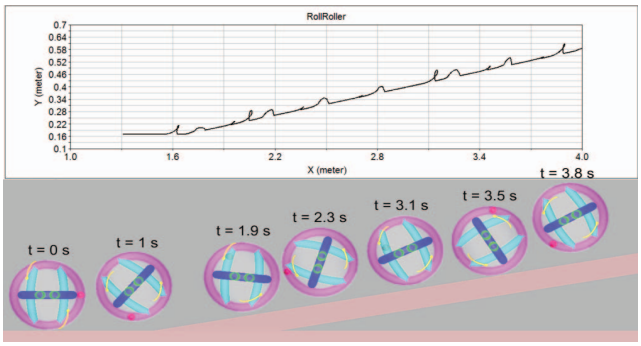

Fig. 12. The robot with algorithm at 10^o incline in simulation space.

different angles for three basic inputs. Here, $R_s = \frac{L_t}{L_s}$ is the fraction of L_t (the traveled distance of robot respecting the slope) to the L_s (the slope total length). The plotted graphs represent direct relation of travel ratio with different torque inputs. As can be seem, the high torque input out-performs traveling distance from the rest of inputs. Steeper angles, more than 17^o, result in a smaller traveling distance the lower torque inputs. It can be seen for all the settings, 17^o angle is the critical point since R_s drops below 5% for all the torque inputs. The Fig. 10 compares the three torque inputs at the critical point $\phi = 17^o$.

B. Hybrid Actuation

Hybrid actuation is implemented with the intermediate torque input. First, we see the performance of the algorithm for the traversable slope angle ($\phi = 10^o$). The Y axis plot in Fig. 11 shows how the hybrid actuation algorithm, based on the use of the GB pipes, rectifies wavy forms of the locomotion and prevents the robot to have many jumps (approximately 50 % decrease in swings). Also, the robot keeps its negative displacement along X axis to minimum, which creates a semi-linear motion. As a negative effect, about 2 sec delay is observed during the propulsion to the end of the slope and falls. At the latest points (basic actuation $7 < t < 8$ sec and hybrid actuation $10 < t < 12$ sec), the the basic actuation creates high peak fluctuation after falling but the hybrid actuation control helps the robot to minimize its interactive jumps. The corresponding behavior is captured along X-Y plot in Fig. 12.

Next, 15^o angle is evaluated to find out the sensitivity of the algorithm to steeper angles (see Fig. 13]). By using the hybrid actuation, RollRoller robot can improve the locomotion at certain intervals of both X and Y axes. However, as time reaches to $t = 5$ sec, the robot is wrong-headed on the slope. To see how robot moves in generic form, the three dimensional plot for three basic slopes are presented in Fig. 14. It becomes clear that the robot loses its direct locomotion and starts following path in Z direction. Therefore, the algorithm requires the use of the turner tube to prevent the robot to follow the off-road.

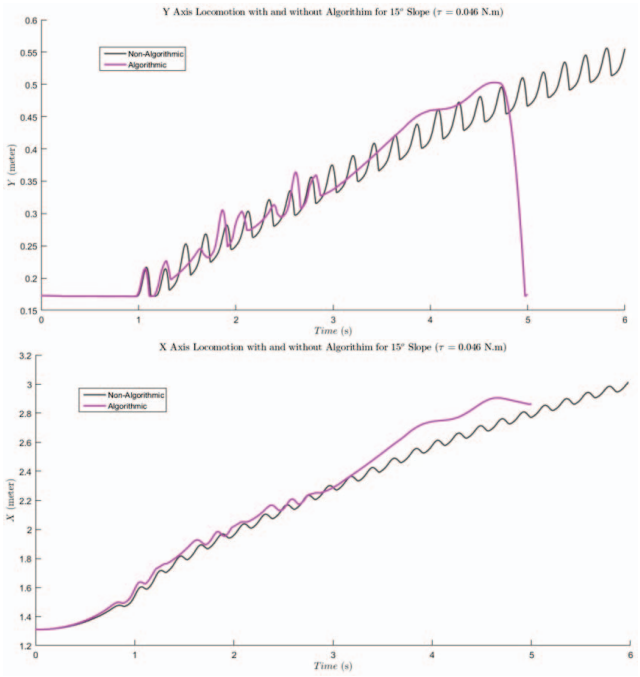

Fig. 13. Y and X axes locomotion with algorithm in 15^o when input torque is intermediate.

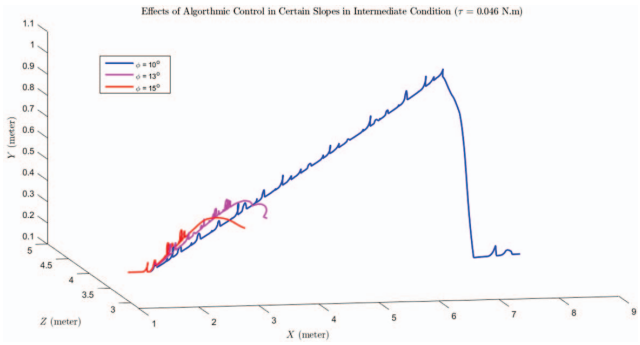

Fig. 14. 3D plot of three algorithmic base locomotion of RollRoller.

V. CONCLUSIONS

The climbing motion of RollRoller robot on the inclined plane was studied under simulation. In the basic actuation, as the torque input increases, the traversable distance rises proportionally. This result is caused by increasing angular momentum. Depending on the achieved motions, the robot is able to climb the slope from 0^o to 17^o without backward displacement. The jump impulses in the basic actuation can be ameliorated by using a hybrid actuation via inclusion of the GB pipes. Despite the essential improvement in latitude jumping and negative backward locomotion, RollRoller is able to keep its direct climbing up to maximum 13^o of the tilted plane. The overall locomotion in this method is represented as a semi-linear displacement on the slope. However, the hybrid actuation has a small delay compared to the basic actuation. It can be concluded that the hybrid actuation can be utilized in situations where the slopes are lower but the slippage is high. Also, it is less safe for the robot to have jumping impulses during its locomotion. In the future research, we plan to create a 3D model control over the RollRoller with including turner tubes to overcome steeper planes.

REFERENCES

[1] R. H. Armour and J. F. Vincent, "Rolling in nature and robotics: A review," *Journal of Bionic Engineering*, vol. 3, no. 4, pp. 195 – 208, 2006.

[2] A. Behar, J. Matthews, F. Carsey, and J. Jones, "Nasa/jpl tumbleweed polar rover," *in Proc. IEEE Aerospace Conf.*, vol. 1, p. 395, March 2004.

[3] J. Asama, M. R. Burkhardt, F. Davoodi, and J. W. Burdick, "Design investigation of a coreless tubular linear generator for a moball: A spherical exploration robot with wind-energy harvesting capability," *in Proc. IEEE Int. Conf. on Robot. and Autom.*, pp. 244–251, May 2015.

[4] A. Halme, T. Schonberg, and Y. Wang, "Motion control of a spherical mobile robot," *in Proc. 4th Int. Workshop Adv. Motion Control (AMC 1996)*, vol. 1, pp. 259–264, Mar 1996.

[5] A. Bicchi, A. Balluchi, D. Prattichizzo, and A. Gorelli, "Introducing the "sphericle": an experimental testbed for research and teaching in nonholonomy," *Proc. IEEE Conf. Robot. Autom.*, vol. 3, pp. 2620–2625, Apr 1997.

[6] C. Wei-Hsi, C. Ching-Pei, Y. Wei-Shun, L. Chang-Hao, and L. Pei-Chun, "Design and implementation of an omnidirectional spherical robot omnicron," *IEEE/ASME Int. Conf. Adv. Intell. Mechatron. (AIM)*, pp. 719–724, July 2012.

[7] A. H. J. A and P. Mojabi, "Introducing august: a novel strategy for an omnidirectional spherical rolling robot," *in Proc. IEEE Int. Conf. on Robot. and Autom.*, vol. 4, pp. 3527–3533, 2002.

[8] J. Brown, H.B. and Y. Xu, "A single-wheel, gyroscopically stabilized robot," *in Proc. IEEE Int. Conf. on Robot. and Autom.*, vol. 4, pp. 3658–3663, Apr 1996.

[9] S. Bhattacharya and S. Agrawal, "Spherical rolling robot: a design and motion planning studies," *IEEE Trans. Robot. Autom.*, vol. 16, no. 6, pp. 835–839, Dec 2000.

[10] G. C. Schroll, "Design of a spherical vehicle with flywheel momentum storage for high torque capabilities," Master's thesis, Massachusetts Institute of Technology, Cambridge, 2008.

[11] D. Liu, H. Sun, and Q. Jia, "Stabilization and path following of a spherical robot," *Proc. IEEE Conf. Robot. Autom. and Mechatron.*, pp. 676–682, Sept 2008.

[12] M. Ishikawa, R. Kitayoshi, and T. Sugie, "Volvot : A spherical mobile robot with eccentric twin rotors," *IEEE Int. Conf. on Robot. and Biom. (ROBIO)*, pp. 1462–1467, Dec 2011.

[13] T. Yu, H. Sun, Q. Jia, Y. Zhang, and W. Zhao, "Stabilization and control of a spherical robot on an inclined plane," *Res. J. Appl. Sci. Eng. Technology*, p. 2289–2296, May 2013.

[14] W.-H. Chen, C.-P. Chen, J.-S. Tsai, J. Yang, and P.-C. Lin, "Design and implementation of a ball-driven omnidirectional spherical robot," *Mechanism and Machine Theory*, vol. 68, pp. 35 – 48, 2013.

[15] F. R. Hogan and J. R. Forbes, "Modeling of spherical robots rolling on generic surfaces," *Multibody System Dynamics*, vol. 35, no. 1, pp. 91–109, 2015.

[16] S. A. Tafrishi, ""RollRoller" novel spherical mobile robot basic dynamical analysis and motion simulations," Master's thesis, University of Sheffield, Sheffield, UK, Sep. 2014.

[17] S. A. Tafrishi, S. M. Veres, E. Esmaeilzadeh, and M. Svinin, "Dynamical behavior investigation and analysis of novel mechanism for simulated spherical robot named "RollRoller"," *Mechanism and Machine Theory*, 2016, under review, Available at https://arxiv.org/abs/1610.06218

[18] S. Mahboubi, M. Seyyed Fakhrabadi, and A. Ghanbari, "Design and implementation of a novel spherical mobile robot," *J. Intell. Robot. Sys.*, vol. 71, no. 1, pp. 43–64, 2012.